

Cite this: *J. Mater. Chem. C*, 2015, 3, 607

# Synthesis of narrow-band red-emitting $\text{K}_2\text{SiF}_6:\text{Mn}^{4+}$ phosphors for a deep red monochromatic LED and ultrahigh color quality warm-white LEDs†

Ji Hye Oh, Heejoon Kang, Yun Jae Eo, Hoo Keun Park and Young Rag Do\*

In this study, we synthesized and characterized narrow-band red-emitting  $\text{K}_2\text{SiF}_6:\text{Mn}^{4+}$  phosphors in order to improve the color qualities of warm white light-emitting diodes (LEDs). The deep red monochromatic LED was realized by fabricating a long wavelength pass dichroic filter (LPDF)-capped phosphor-converted LED (pc-LED) with a synthesized  $\text{K}_2\text{SiF}_6:\text{Mn}^{4+}$  phosphor. In addition, we introduced four-package white LEDs that combine InGaN blue (B) LED and LPDF-capped green (G), amber (A), and red (R) pc-LEDs to achieve the high color rendition at the warm white correlated color temperatures (CCTs, 2700 K) with the assistance of the narrow-band  $\text{K}_2\text{SiF}_6:\text{Mn}^{4+}$  red phosphor. We compared the optical properties, including the luminous efficacy (LE), luminous efficacy of radiation (LER), color rendering index (CRI), special CRI for strong red ( $R_9$ ), and color quality scale (CQS), of four-package white LEDs by varying the red pc-LED with one narrow-band red-emitting phosphor and five wide-band red-emitting phosphors. The RAGB four-package white LED using narrow-band red-emitting  $\text{K}_2\text{SiF}_6:\text{Mn}^{4+}$  phosphor exhibited high LE ( $107 \text{ lm W}^{-1}$ ) and ultrahigh color qualities (CRI = 94,  $R_9$  = 93, and CQS = 93) at a CCT of 2700 K.

Received 11th September 2014  
Accepted 10th November 2014

DOI: 10.1039/c4tc02042a

www.rsc.org/MaterialsC

## 1. Introduction

White-color phosphor-converted light-emitting diodes (pc-LEDs) are an attractive white lamp technology compared with the currently commercialized lighting, such as incandescent and fluorescent lamps, due to the pc-LED's distinct advantages of high efficiency, eco-friendliness (mercury-free composition), long lifetime, small size, high brightness, facile fabrication, and fast response times, which are offered by this type of lighting.<sup>1,2</sup> In pc-LEDs, the white light is obtained simply *via* a combination of leaked blue emissions through the phosphor layer from a blue LED chip and the broad green-yellow emission of yellow (Y) phosphors, or the combined multi-color emissions of green/red (G/R) or green/amber/red (G/A/R) phosphors.<sup>3–5</sup> In general LED lighting systems, warm white indoor illumination and a higher color rendering index (CRI;  $R_a > 90$ ) are needed at a low correlated color temperature (CCT) of 2700 K to retrofit the incandescent tungsten-halogen lamps (CRI = 100, CCT =  $\sim 2812$  K) in the market.<sup>3</sup> However, most single package white pc-LEDs, including the tri-phosphor approach (*i.e.* a combination of G, A, and R phosphors), cannot achieve high CRIs ( $R_a > 88$ ), while using a series of currently commercialized nitride red phosphors that are broad band (Ca,Sr)AlSiN<sub>3</sub>:Eu<sup>2+</sup> phosphors (peak

wavelength ( $\lambda_{em}$ ) = 610–660 nm, full-width at half-maximum (FWHM) > 85 nm, SCASIN family).<sup>6</sup>

To date, the best single phosphor-single package approach achieves a warm white emission with CCT < 4000 K, CRI > 80 and luminous efficacy (LE) of  $20 \text{ lm W}^{-1}$  when combining the wide-band Ba<sub>0.93</sub>Eu<sub>0.07</sub>Al<sub>2</sub>O<sub>4</sub> yellow phosphor with a blue LED.<sup>4</sup> For the multi-color-single package approaches, two types of narrow-band red phosphors have been recently developed to achieve a higher CRI for the warm white pc-LEDs than the pc-LEDs with wide-band nitride red phosphors.<sup>7–10</sup> Here, narrow-band red phosphors are required to satisfy the spectral power distribution (SPD) of the Planckian locus, which is the reference chromaticity below a CCT of 5000 K. First, a CRI of 90.9 and LE of  $81.56 \text{ lm W}^{-1}$  at a CCT of 3510 K was obtained by combining the wide-band Y<sub>3</sub>Al<sub>5</sub>O<sub>12</sub>:Ce<sup>3+</sup> yellow with the narrow-band  $\text{K}_2\text{SiF}_6:\text{Mn}^{4+}$  red phosphor (FWHM  $\sim 10$  nm of the main peak) on a blue LED.<sup>7</sup> Second, a CRI of 91 at a CCT of 2700 K was recently reached by fabricating a mixture of Lu<sub>3</sub>Al<sub>5</sub>O<sub>12</sub>:Ce<sup>3+</sup> green phosphor, (Ba,Sr)<sub>2</sub>Si<sub>5</sub>N<sub>8</sub>:Eu<sup>2+</sup> orange phosphor, and the new narrow-band SrLiAl<sub>3</sub>N<sub>4</sub>:Eu<sup>2+</sup> red phosphor (FWHM  $\sim 50$  nm) on a blue LED.<sup>9</sup>

Because the CRI value is calculated using the eight pastel series of test color samples, a high CRI cannot guarantee good saturated colors of a light source.<sup>11</sup> For this reason, the other values are needed in order to evaluate the color quality in not only the pastel series of colors but also the saturated series of RGB colors. Therefore, the special CRI for a strong red ( $R_9$ ) and color quality scale (CQS), which is calculated using 15 reflective

Department of Chemistry, Kookmin University, Seoul 136-702, Korea. E-mail: yrdo@kookmin.ac.kr; Tel: +82-2-910-4893

† Electronic supplementary information (ESI) available. See DOI: 10.1039/c4tc02042a

Munsell samples and a saturation factor, were recently proposed in order to achieve high color quality in the light source.<sup>11–14</sup> The development of a warm white LED with excellent color qualities for the three indicators (CRI,  $R_a \geq 90$ ,  $R_9 \geq 90$  and CQS,  $Q_a \geq 90$ ) remains a challenge for the solid-state LED lighting industry without reducing the energy efficiency in order to perfectly retrofit incandescent tungsten–halogen lamps.

Recently, we created a series of  $R_{B,M}A_{B,M}G_{B,M}B$  four color–four package white LEDs that have high luminous efficacies ( $LEs > 90 \text{ lm W}^{-1}$ ) and high CRIs ( $>85$ ) in the color emission range between a cool white (6500 K) color to a warm white (2700 K) color. Here,  $R_{B,M}A_{B,M}G_{B,M}B$  represents long wavelength pass dichroic filter (LPDF)-capped, monochromatic red ((Sr,Ca)AlSiN<sub>3</sub>:Eu<sup>2+</sup>), amber ((Ba,Ca,Sr)<sub>3</sub>SiO<sub>5</sub>:Eu<sup>2+</sup>), and green ((Ba,Ca,Sr)<sub>n</sub>SiO<sub>4</sub>:Eu<sup>2+</sup>) pc-LEDs pumped by a blue LED chip. B denotes an InGaN blue LED. The most remarkable feature of our  $R_{B,M}A_{B,M}G_{B,M}B$  four package LEDs is that the various figures of merits of the white LEDs pertaining to the circadian performances, as well as the vision performances and color qualities, are controlled and optimized by changing the types of phosphors in order to create high quality smart lighting systems for human health, energy savings, and the realization of natural colors, while the LEDs are tuned from a cool white to a warm white color.<sup>15</sup>

In this study, first, we synthesized the recently proposed narrow-band  $K_2SiF_6:Mn^{4+}$  phosphors using a facile etching synthetic process and characterize their crystal, morphological, and optical properties. Next, we fabricated LPDF-capped red/amber/green full down-converted monochromatic pc-LEDs using purchased G, A, wide-band R phosphors, and prepared narrow-band R phosphors. Finally, we demonstrate a  $R_{B,M}A_{B,M}G_{B,M}B$  four package white LED system that consists of a narrow-band red phosphor ( $K_2SiF_6:Mn^{4+}$ ) pc-LED, wide-band G/A pc-LEDs, and a blue LED in an effort to enhance the all CRI,  $R_9$ , and CQS of warm white light over 90 at a CCT of 2700 K, and to dynamically control the color points without sacrificing energy efficiency. In detail, we also compare the color performances (CRI,  $R_9$ , and CQS) and visual energy performances (LE and luminous efficacy of radiation (LER)<sup>16</sup>) of the four package color-mixing white LEDs including a narrow-band red phosphor and a series of wide-band red phosphors ((Sr,Ca)AlSiN<sub>3</sub>:Eu<sup>2+</sup>) as a function of the CCT in the range of 2000–6500 K in order to evaluate the feasibility of multi-package LEDs as an excellent warm white lighting source, as well as a smart tunable lighting source.

## 2. Experimental

### 2.1. Fabrication of LPDFs<sup>15,17–19</sup>

For the design of the LPDF multilayer film, the characteristic matrix method was used to simulate the reflectance, transmittance, and absorption as a function of the thickness of high and low index films. For the stack fabrication, terminal one-eighth-wave-thick TiO<sub>2</sub> and quarter-wave-thick SiO<sub>2</sub> nanomultilayered films (0.5TiO<sub>2</sub>/SiO<sub>2</sub>/0.5TiO<sub>2</sub>)<sup>9</sup> were coated onto glass substrates *via* e-beam evaporation at 250 °C. The

transmittance and reflectance spectra of the LPDFs were optimized by changing the thickness of the TiO<sub>2</sub> and SiO<sub>2</sub> layers. The L535 (25/73/25 nm)<sup>9</sup> was the green pc-LED and L550 (26/73/26 nm)<sup>9</sup> was the amber and red pc-LEDs. Fig. S1† illustrates the transmittance of both L535 and L550 LPDFs and provides photographs of the transmission and reflection of a L535 LPDF. The transmittance spectra of the LPDFs were measured using a UV-vis spectrophotometer (S-3100, Sinco Co., Ltd) (see Fig. S1†).

### 2.2. Synthesis of red-emitting $K_2SiF_6:Mn^{4+}$ phosphor<sup>7</sup> and characterization of powder phosphors

A schematic diagram of the synthesis method of red-emitting  $K_2SiF_6:Mn^{4+}$  is shown in Fig. 1a. In order to synthesize the red-emitting  $K_2SiF_6:Mn^{4+}$  phosphor, pure SiO<sub>2</sub> powders were dissolved in HF (25 vol%) at room temperature for 2 hours to form a H<sub>2</sub>SiF<sub>6</sub> solution. A stoichiometric amount of KMnO<sub>4</sub> was dissolved in the H<sub>2</sub>SiF<sub>6</sub> solution. After the color of the solution changed from colorless to a deep purple, H<sub>2</sub>O<sub>2</sub> (30 vol%) was added drop-by-drop. The solution formed a yellow precipitate of  $K_2SiF_6:Mn^{4+}$  powders. After completion of the reaction, the powders were filtered and dried at 80 °C in the oven. The emission and excitation of all powder phosphors were measured using a Xe-lamp and spectrophotometer (Darsa, PSI Trading Co., Korea). The internal and external quantum efficiencies of all powder phosphors were measured using a half-moon-based quantum efficiency measurement system (Otsuka Electronics). The crystal structure of the  $K_2SiF_6:Mn^{4+}$  phosphor was investigated *via* X-ray diffraction with CuK<sub>α1</sub> radiation (D-max 2500, JEOL, USA) with JCPDS 85-1382 ( $K_2SiF_6$ ). The morphology of the  $K_2SiF_6:Mn^{4+}$  phosphor was measured using field emission scanning electron microscopy (FE-SEM) including energy-dispersive X-ray spectroscopy (EDS) (JEM-7610F, JEOL, Japan).

### 2.3. Fabrication of $G_{B,M}$ , $A_{B,M}$ , and $R_{B,M}$ monochromatic pc-LEDs<sup>15,17–19</sup>

LPDF-capped, monochromatic G/A/R pc-LEDs were fabricated using green ((Ba,Ca,Sr)<sub>n</sub>SiO<sub>4</sub>:Eu<sup>2+</sup>), amber ((Ba,Ca,Sr)<sub>3</sub>SiO<sub>5</sub>:Eu<sup>2+</sup>), narrow-band red ( $R_N$ ,  $K_2SiF_6:Mn^{4+}$ ), and five types of wide-band red ( $R1_W$ ,  $R2_W$ ,  $R3_W$ ,  $R4_W$ , and  $R5_W$ , (Sr,Ca)AlSiN<sub>3</sub>:Eu<sup>2+</sup>; SCASIN family) phosphors. The wide-band G/A/R phosphors were purchased from Intematix Corporation (USA). An InGaN blue LED was used as an excitation source for various R, A, and G color phosphors. The blue LED packages were purchased from Dongbu LED, Inc. (Korea). The optimum amount of G/A/R phosphors were dispersed in a silicon binder (OE-6636A,B, Dow Corning, USA) and the phosphor pastes were dropped onto a cup-type blue LED package. The phosphor pastes were hardened in an oven at 150 °C for one hour. Then, the LPDF was simply capped on the LED package in order to realize the  $G_{B,M}$ ,  $A_{B,M}$ , and  $R_{B,M}$  pc-LEDs. The LPDF-capped monochromatic narrow-band red pc-LED is denoted as  $R_{N,B,M}$  pc-LED, and the five types of wide-band red pc-LEDs are denoted as  $R1_{W,B,M}$ ,  $R2_{W,B,M}$ ,  $R3_{W,B,M}$ ,  $R4_{W,B,M}$ , and  $R5_{W,B,M}$  pc-LEDs.

#### 2.4. Characterization of $G_{B,M}$ , $A_{B,M}$ , and $R_{B,M}$ monochromatic pc-LEDs and four-package $R_{B,M}A_{B,M}G_{B,M}B$ white LEDs<sup>15,17–19</sup>

The optical properties of an InGaN semiconductor-type blue LED and  $G_{B,M}$ ,  $A_{B,M}$ , and  $R_{B,M}$  pc-LEDs were measured in an integrated sphere with an applied current of 250 mA using a spectrometer (Darsapro-5000, PSI Trading Co., Korea). The optical properties of the  $R_{B,M}A_{B,M}G_{B,M}B$  white LEDs were also measured by placing the four package into a square lattice fixture in an integrated sphere using a spectrometer (Darsapro-5000, PSI Trading Co., Korea). Six combinations of four-package  $R_{B,M}A_{B,M}G_{B,M}B$  white LEDs were measured with variations of  $R_{B,M}$  pc-LEDs ( $R_{N,B,M}$  pc-LED and five types of  $R1_{W,B,M}$ ,  $R2_{W,B,M}$ ,  $R3_{W,B,M}$ ,  $R4_{W,B,M}$ , and  $R5_{W,B,M}$  pc-LEDs) at different CCTs (2000 K, 2700 K, 3000 K, 3500 K, 5000 K, and 6500 K) by controlling the applied current of the primary pc-LEDs (B LED and  $R_{B,M}$ ,  $A_{B,M}$ , and  $G_{B,M}$  pc-LEDs) with a total applied current of 1000 mA. The temperature dependences of the optical properties were also measured using a heating die from room temperature to 120 °C.

### 3. Results and discussion

$K_2SiF_6:Mn^{4+}$  phosphors were synthesized using a facile etching method that has been reported previously (see Fig. 1a).<sup>7,8,20,21</sup> Fig. 1b presents the excitation and emission spectra of the as-prepared  $K_2SiF_6:Mn^{4+}$  phosphors. It demonstrates that the typical absorption bands are attributed to the  $^4A_2-^4T_{1,2}$  transitions of  $Mn^{4+}$  in the UV and blue regions. The emission spectrum of our sample had five sharp peaks that resulted from the  $^2E_2-^4A_1$  transitions of  $Mn^{4+}$  in the  $K_2SiF_6:Mn^{4+}$  phosphors.

The strong PL emission revealed that five narrow emission peaks ( $\sim 609$  ( $\nu_4$ ),  $\sim 613$  ( $\nu_6$ ),  $\sim 630$  ( $\nu_6$ ),  $\sim 635$  ( $\nu_4$ ), and  $\sim 648$  nm ( $\nu_3$ )) were a typical property of  $Mn^{4+}$  ion-activated phosphors as reported previously.<sup>20</sup> As seen in Fig. 1c, the powder XRD data demonstrate that all diffraction peaks of the as-synthesized  $K_2SiF_6:Mn^{4+}$  phosphors could be indexed to the cubic  $K_2SiF_6$  (JCPDS card no. 85-1382) single phase without impurity phases. The SEM picture illustrates that micrometer-sized powders with irregular round shapes were observed in the as-synthesized

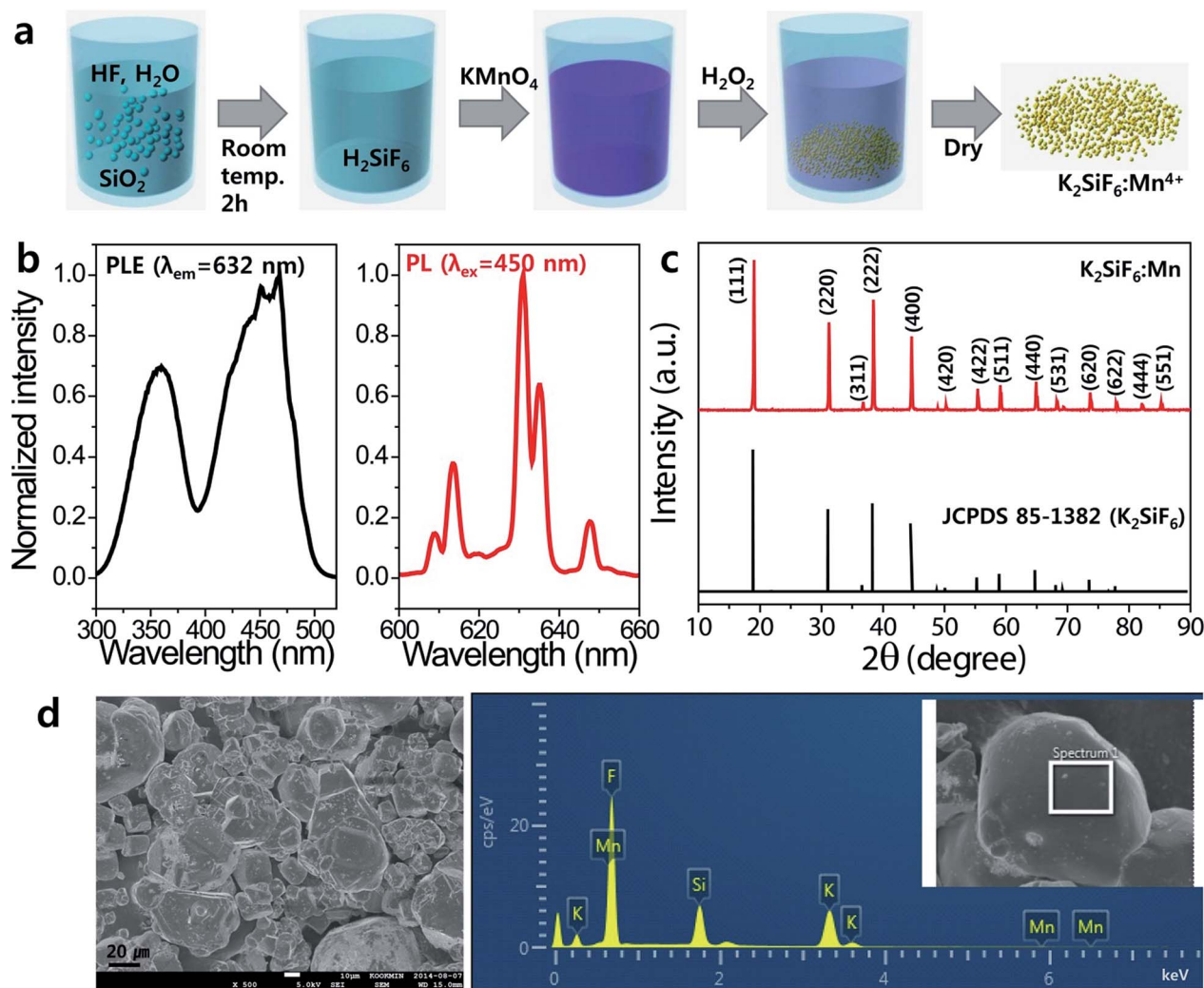


Fig. 1 (a) Schematic diagram of the synthetic method of  $K_2SiF_6:Mn^{4+}$ , (b) the excitation and emission spectra, (c) powder XRD (JCPDS 85-1382 ( $K_2SiF_6$ )), and (d) FE-SEM and EDS data of the as-synthesized  $K_2SiF_6:Mn^{4+}$  phosphor.

$\text{K}_2\text{SiF}_6:\text{Mn}^{4+}$  phosphors. The EDS clearly identifies peaks of F, Si, K, and Mn elements. As seen in Fig. 1c and d, the XRD and FE-SEM including the EDS data confirm that the crystal qualities, morphologies, and chemical composition of the synthesized  $\text{K}_2\text{SiF}_6:\text{Mn}^{4+}$  phosphors were well matched with those reported in previous publications.<sup>7</sup>

It is necessary to analyze whether the narrow band spectrum of a red phosphor is more apt to achieve high efficiency and high level of color quality for application in monochromatic red and white pc-LEDs. Table 1 summarizes the optical properties of the narrow-band  $\text{K}_2\text{SiF}_6:\text{Mn}^{4+}$  phosphor and a series of wide-band (Sr,Ca)AlSiN<sub>3</sub>:Eu<sup>2+</sup> (SCASIN) phosphors. For convenience, in this study, R<sub>N</sub> denotes the narrow-band  $\text{K}_2\text{SiF}_6:\text{Mn}^{4+}$  phosphor and R1<sub>W</sub>–R5<sub>W</sub> denote the SCASIN phosphor series with increases in the dominant wavelength (DWL). The internal and external quantum efficiency (QE) of the as-prepared  $\text{K}_2\text{SiF}_6:\text{Mn}^{4+}$  phosphor remained lower than the corresponding wide-band R5<sub>W</sub> red phosphor at similar CIE color coordinates because the SCASIN phosphors have been well optimized over a long time and are commercialized. Although we optimized the properties of the  $\text{K}_2\text{SiF}_6:\text{Mn}^{4+}$  phosphor in the laboratory, it is necessary to further improve the QE of the narrow-band  $\text{K}_2\text{SiF}_6:\text{Mn}^{4+}$  phosphor in order to satisfy the properties required for commercial purposes. Fig. 2 presents the normalized photoluminescence (PL) spectra and color coordinates of six red phosphors excited by blue light. Fig. 2a also includes the photopic luminosity function ( $V(\lambda)$ ), which indicates the average spectral sensitivity of the visual brightness perceived by the retina cone cells in human eyes under bright light levels. As reported,<sup>22</sup> the red-shift behavior of the SCASIN phosphors can be interpreted in terms of the increased crystal field strength around the Eu<sup>2+</sup> ions. The luminous efficacy of radiation (LER) and relative brightness of the SCASIN phosphor family decreased with increases in the maximum peak wavelength due to the decrease of overlapping with the  $V(\lambda)$  spectrum. This clearly indicates that the deep red emissions of the SCASIN phosphors above ~690 nm waste photons due to the vision performance of humans.

Therefore, the emitted photons of red phosphors above ~700 nm do not affect the perceived brightness and color discrimination in human eyes. The waste photon ratio (WPR) of red phosphors can be defined as the ratio between the number

of photons emitted from phosphors above ~700 nm and the total number of photons from the phosphors excited by blue light. The deepest wide-band red SCASIN phosphor (R5<sub>W</sub>,  $\lambda_{\text{max}} = 670$  nm) wastes approximately 12% of emitted photons, otherwise almost 100% of photons emitted from the narrow-band  $\text{K}_2\text{SiF}_6:\text{Mn}^{4+}$  phosphors are utilized by the human eye. For these reasons, the relative brightness of the narrow-band red phosphor appears to be 2.7-fold higher than the deepest R5<sub>W</sub> phosphor in all five wide-band red phosphors at similar 1931 Commission Internationale d'Eclairage (CIE)  $x, y$  color coordinates. As seen in Fig. 2b, the color coordinates of the  $\text{K}_2\text{SiF}_6:\text{Mn}^{4+}$  phosphors are located at the deep red point in the CIE color diagram. Although the absolute QE of the as-synthesized  $\text{K}_2\text{SiF}_6:\text{Mn}^{4+}$  phosphor was lower than the wide-band SCASIN phosphor at the corresponding CIE color coordinates, the excellent brightness and deep red color of the narrow-band red phosphor could be realized for application in red pc-LEDs. The next step is to fabricate a monochromatic red pc-LED using a narrow-band phosphor. The deep red color of the LPDF-capped pc-LED with the  $\text{K}_2\text{SiF}_6:\text{Mn}^{4+}$  phosphor can be realized through simply capping the LPDF on top of the InGaN blue LED deposited and varying the concentrations of  $\text{K}_2\text{SiF}_6:\text{Mn}^{4+}$  phosphors in a paste. As depicted in Fig. S2,<sup>†</sup> with the increase of the  $\text{K}_2\text{SiF}_6:\text{Mn}^{4+}$  red phosphor concentration, the LE of the red pc-LED increased and the blue portion of the red pc-LED decreased. Therefore, 50 wt% of the phosphors, the minimum amount of full-color conversion in the LPDF-capped pc-LED, were carefully selected in order to guarantee the maximum level of luminous efficacy, color purity, and 1931 CIE color

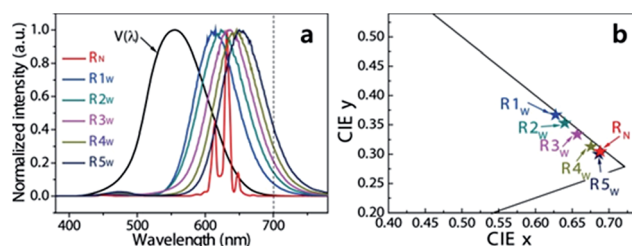


Fig. 2 (a) The photopic luminosity function ( $V(\lambda)$ ) and normalized PL spectra of six red phosphors and (b) the 1931 color coordinates of the six red phosphors.

Table 1 The optical properties of phosphors

Phosphor	Color coordinates	Absolute quantum efficiency		Band-width (nm)	DWL (nm)	Color purity	WPR (%)		
		External	Internal						
G	(Ba,Ca,Sr) <sub>n</sub> SiO <sub>4</sub> :Eu	0.286	0.645	0.62	0.81	65.3	523	78	0
A	(Ba,Ca,Sr) <sub>3</sub> SiO <sub>5</sub> :Eu	0.582	0.414	0.69	0.82	78.4	603	98	1
R <sub>N</sub>	$\text{K}_2\text{SiF}_6:\text{Mn}$	0.688	0.305	0.54	0.80	8.4	632	98	0
R1 <sub>W</sub>	(Sr,Ca)AlSiN <sub>3</sub> :Eu	0.627	0.367	0.64	0.91	88.0	621	99	2
R2 <sub>W</sub>	(Sr,Ca)AlSiN <sub>3</sub> :Eu	0.640	0.353	0.65	0.91	93.4	635	97	4
R3 <sub>W</sub>	(Sr,Ca)AlSiN <sub>3</sub> :Eu	0.657	0.334	0.64	0.92	88.2	650	97	5
R4 <sub>W</sub>	(Sr,Ca)AlSiN <sub>3</sub> :Eu	0.676	0.313	0.71	0.90	87.6	657	97	8
R5 <sub>W</sub>	(Sr,Ca)AlSiN <sub>3</sub> :Eu	0.686	0.300	0.73	0.86	91.0	664	96	12

coordinates similar to those of the corresponding  $\text{K}_2\text{SiF}_6:\text{Mn}^{4+}$  powder.

Fig. 3a shows the schematic diagram of the four-package white LED and Fig. 3b to d present the electroluminescence (EL) spectra, 1931 CIE color coordinates, and photographs of the blue semiconductor-type LED and eight different colors of full down-converted, LPDF-capped pc-LEDs (one green, one amber, one narrow-band red, and five wide-band reds (SCASIN phosphors)). As shown in Fig. S3† the pc-LEDs without LPDFs show blue emission from the InGaN blue LED and phosphor emission (green, amber, and red). However, the pc-LEDs with LPDFs show full down converted phosphor emission and enhance the emission output because the LPDF reflects and recycles blue emission. Also, we previously reported that, compared to the conventional pc-LEDs (without LPDF), the LPDF-capped pc-LEDs can reduce the phosphor concentration in the silicon binder and enhance the luminous efficacy by reducing the

scattering loss from the phosphor layer.<sup>17</sup> Here, a series of wide-band red colors and a narrow-band red color were obtained by varying the type and concentration of the phosphor material in the LPDF-capped pc-LEDs. As seen in Fig. 2a and 3b, the EL emission spectra of all monochromatic pc-LEDs are well matched with those of the corresponding phosphors as previously reported.<sup>13–15</sup> The emitting images also confirm that the deepest red color was obtained using the red pc-LED with a narrow-band red phosphor.

Table 2 summarizes the resultant optical properties of the blue LED and  $\text{G}_{\text{B,M}}$ ,  $\text{A}_{\text{B,M}}$ , and  $\text{R}_{\text{B,M}}$  pc-LEDs used in this experiment (applied current = 250 mA). The table indicates that the LE and LER values of the  $\text{R}_{\text{B,M}}$  pc-LEDs with SCASIN phosphors decreased significantly with increases in the peak wavelength, which is the same as the powder phosphors. The LER and LE trends on the peak wavelength resulted from the appearance of the photopic spectral luminous efficiency function (photopic sensitivity) and wide-band emission spectra of the SCASIN phosphors as described above. The LE and LER of the  $\text{R}_{\text{N,B,M}}$  pc-LED were much higher than those of the  $\text{R}_{5\text{W,B,M}}$  pc-LED at similar 1931 CIE color coordinates, due to the absence of unnecessary emissions in the deep red and IR. This indicates that the  $\text{R}_{\text{N,B,M}}$  pc-LED could be the ideal red monochromatic LED from the perspective of both color coordinates and energy efficiency, although further improvement of QE is necessary for the  $\text{K}_2\text{SiF}_6:\text{Mn}^{4+}$  phosphor.

Fig. S4† presents the current and temperature dependence of the blue LED and  $\text{G}_{\text{B,M}}$ ,  $\text{A}_{\text{B,M}}$ , and  $\text{R}_{\text{B,M}}$  pc-LEDs. We selected the  $\text{R}_{2\text{W,B,M}}$  pc-LED and  $\text{R}_{5\text{W,B,M}}$  pc-LED, which exhibited similar LE/dominant wavelength (DWL) and CIE color coordinates, respectively, in order to compare their current and temperature dependence with the  $\text{R}_{\text{N,B,M}}$  pc-LED. As seen in Fig. S4,† the  $\text{R}_{\text{N,B,M}}$  pc-LED was thermally stable as well as the blue LED. This indicates that the  $\text{K}_2\text{SiF}_6:\text{Mn}^{4+}$  red phosphor is more thermally stable than the green  $((\text{Ba,Ca,Sr})_n\text{SiO}_4:\text{Eu}^{2+})$ , amber  $((\text{Ba,Ca,Sr})_3\text{SiO}_5:\text{Eu}^{2+})$ , and red  $((\text{Sr,Ca})\text{AlSiN}_3:\text{Eu}^{2+})$  SCASIN phosphors.

Finally, four-package  $\text{R}_{\text{B,M}}\text{A}_{\text{B,M}}\text{G}_{\text{B,M}}\text{B}$  white LEDs were prepared and characterized in order to compare the effect of the  $\text{R}_{\text{N,B,M}}$  pc-LED on the optical properties of the four package white LED. The  $\text{R}_{\text{B,M}}\text{A}_{\text{B,M}}\text{G}_{\text{B,M}}\text{B}$  white LED can realize various

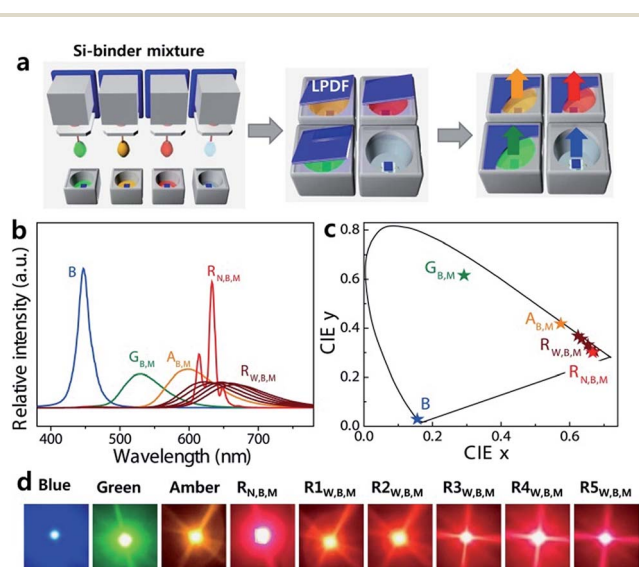


Fig. 3 (a) Schematic diagram of four-package white LED, (b) the EL spectra, (c) 1931 CIE color coordinates, and (d) photographs of the blue semiconductor-type LED and eight different colors of fully down-converted LPDF-capped pc-LEDs ( $\text{G}_{\text{B,M}}$ ,  $\text{A}_{\text{B,M}}$ ,  $\text{R}_{\text{N,B,M}}$ ,  $\text{R}_{1\text{W,B,M}}$ ,  $\text{R}_{2\text{W,B,M}}$ ,  $\text{R}_{3\text{W,B,M}}$ ,  $\text{R}_{4\text{W,B,M}}$ , and  $\text{R}_{5\text{W,B,M}}$ ).

Table 2 The optical properties of blue LED and pc-LEDs

Phosphor weight (%)	Color coordinates		LE ( $\text{lm W}^{-1}$ )	LER ( $\text{lm W}^{-1}$ )	B-W (nm)	DWL (nm)	
	CIE x	CIE y					
B	—	0.156	0.029	14	37	20	447
$\text{G}_{\text{B,M}}$	40	0.292	0.616	173	500	67	529
$\text{A}_{\text{B,M}}$	20	0.574	0.418	127	343	83	598
$\text{R}_{\text{N,B,M}}$	50	0.668	0.303	65	196	10	633
$\text{R}_{1\text{W,B,M}}$	10	0.625	0.369	78	220	91	624
$\text{R}_{2\text{W,B,M}}$	10	0.635	0.356	62	173	97	637
$\text{R}_{3\text{W,B,M}}$	10	0.653	0.332	44	122	93	646
$\text{R}_{4\text{W,B,M}}$	10	0.660	0.314	33	91	97	657
$\text{R}_{5\text{W,B,M}}$	10	0.672	0.304	22	66	101	667

CCTs by tuning the fractional applied current of the primary LEDs in each four package white light.

As seen in Fig. 4, the fractional applied currents of the primary LEDs differed slightly for the six different combinations of the  $R_{B,M}A_{B,M}G_{B,M}B$  white LED at any specified CCT, and the CCT decreased with increases in the fractional radiant flux of the red  $R_{B,M}$  and amber  $A_{B,M}$  pc-LEDs.

We compared the figures of merit for the vision performance and color quality of the  $R_{B,M}A_{B,M}G_{B,M}B$  four-package white LEDs, including a narrow-band  $K_2SiF_6:Mn^{4+}$   $R_{N,B,M}$  pc-LED and five wide-band SCASIN phosphor  $R_{W,B,M}$  pc-LEDs. Fig. 5 presents the measured SPDs in the various  $R_{B,M}A_{B,M}G_{B,M}B$  four-package white LEDs at CCTs of 2000 K (firelight), 2700 K (warm white), 3000 K, 3500 K, 5000 K, and 6500 K (cool white). The  $R_{B,M}A_{B,M}G_{B,M}B$  white LED system with an  $R_{N,B,M}$  pc-LED exhibited a broad green-amber spectrum with narrow peaks in the red regions, while the other systems, combined with  $R_{W,B,M}$  pc-LEDs, exhibited a broad spectrum in the wavelength range between green and red at all CCTs. These figures also indicate that the blue and green portions of the white color decreased with decreases in CCT due to the decreasing fractional applied current of the blue and green pc-LEDs. In contrast, the fractional applied current of the amber and red pc-LEDs increased with decreases in the CCT, irrespective of the bandwidth level of the narrow-band and wide-band red phosphors.

The CRI of any artificial lighting sources can be calculated by measuring the ability of a specific light source to reveal the colors of objects while comparing it with an ideal light source, which is sunlight over 5000 K of CCT and a Planckian locus radiation less than 5000 K of CCT. The SPD shapes of the four-package white LED system with an  $R_{N,B,M}$  pc-LED were similar to that of the Planckian locus with a decrease of CCT to less than

5000 K. Otherwise, the SPD shapes of the four-package white LED system with a wide-band red pc-LED were close to those of the radiation spectrum of sunlight above 5000 K. Therefore, the CRI of the four-package white LED system with a narrow-band red pc-LED had a higher value than that of the four-package white LED with  $R_{W,B,M}$  pc-LED in the warm white color ranges (CCT 2000–3500 K).

Table S1† summarizes the optical properties of the six combinations of four-package white LED lamps at room temperature. Also, Fig. 6 presents the LE, LER, CRI,  $R_9$ , and CQS of the six combinations of  $R_{B,M}A_{B,M}G_{B,M}B$  white LEDs at different CCTs with the variations in the red phosphors. As seen in Table S1† and Fig. 6, the  $R_{B,M}A_{B,M}G_{B,M}B$  white LED with the  $R_{N,B,M}$  pc-LED was superior not only in terms of the LE and LER values, but also in terms of the CRI,  $R_9$ , and CQS at all CCTs to the four-package white LED with  $R_{W,B,M}$  pc-LEDs. Although  $R_{N,B,M}$  and  $R_{2,W,B,M}$  red pc-LEDs have similar LEs and DWLs, the LE of  $R_{N,B,M}A_{B,M}G_{B,M}B$  white LED was higher than that of  $R_{2,W,B,M}A_{B,M}G_{B,M}B$  white LED because the fractional applied current of  $A_{B,M}$  and  $R_{B,M}$  pc-LEDs shows different patterns between  $R_{N,B,M}$  and  $R_{W,B,M}$  pc-LEDs. Furthermore, the color qualities of the  $R_{2,W,B,M}A_{B,M}G_{B,M}B$  white LED were significantly lower than those of the  $R_{N,B,M}A_{B,M}G_{B,M}B$  white LED. Even for the  $R_{5,W,B,M}A_{B,M}G_{B,M}B$  white LED with the deepest wide-band red phosphor, the color qualities were lower than those of the  $R_{N,B,M}A_{B,M}G_{B,M}B$  white LED with a narrow-band red phosphor at all CCTs (2000–6500 K). Furthermore, the optical properties of the four-package  $R_{N,B,M}A_{B,M}G_{B,M}B$  white LED including the narrow-band red pc-LED exhibited the best values in all CCTs in comparison with the four-package  $R_{W,B,M}A_{B,M}G_{B,M}B$  white LED, including the series of wide-band SCASIN phosphors.

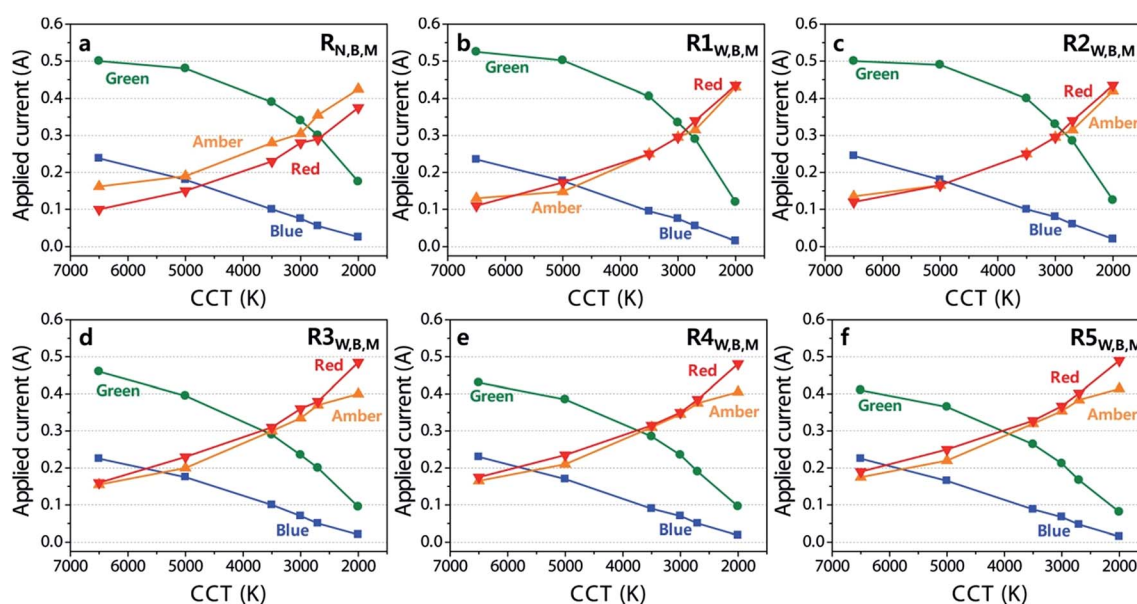


Fig. 4 The fractional applied currents of the primary LEDs in six combinations of a four-package  $R_{B,M}A_{B,M}G_{B,M}B$  white LED at different CCTs with the various red phosphors: (a)  $R_{N,B,M}$ , (b)  $R_{1,W,B,M}$ , (c)  $R_{2,W,B,M}$ , (d)  $R_{3,W,B,M}$ , (e)  $R_{4,W,B,M}$ , and (f)  $R_{5,W,B,M}$ .

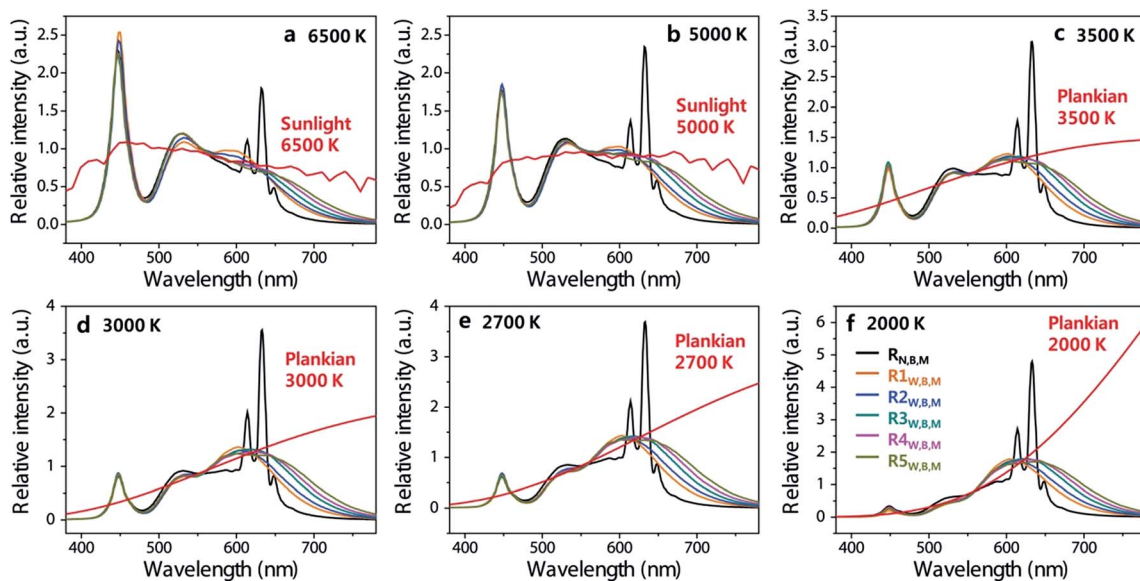


Fig. 5 The EL spectra of the six combinations of four-package  $R_{B,M}A_{B,M}G_{B,M}$  white LEDs at different CCTs with the various red phosphors and the reference ideal (Planckian) or natural (sunlight) light sources of CRI at different CCTs: (a) 6500 K, (b) 5000 K, (c) 3500 K, (d) 3000 K, (e) 2700 K, and (f) 2000 K.

Fig. 7 presents the current and temperature dependence of the four-package  $R_{N,B,M}A_{B,M}G_{B,M}$  white LED at a CCT of 2700 K. The LERs of the  $R_{N,B,M}A_{B,M}G_{B,M}$  white LED decreased from  $123 \text{ lm W}^{-1}$  to  $83 \text{ lm W}^{-1}$  and from  $98 \text{ lm W}^{-1}$  to  $78 \text{ lm W}^{-1}$ , with increases in the applied current from 250 to 1500 mA at room temperature and the temperature from 25 to  $100^\circ\text{C}$  at 1000 mA, respectively. Furthermore, the LER, CRI, and CCT exhibited almost constant values with increases in the current and temperature. These constant current and temperature dependences of the CCTs of the four-package  $R_{N,B,M}A_{B,M}G_{B,M}$  white

LED with a narrow-band red pc-LED confirm that all green, amber, and red pc-LEDs and the blue LED have similar current and temperature dependences in the applied currents. Therefore, these figures confirm that the four-package  $R_{N,B,M}A_{B,M}G_{B,M}$  white LED with a narrow-band red phosphor has acceptable variations of LE, LER, CCT, and CRI with increases in both the applied current and the ambient temperature; these variation trends are similar to those of four-package  $R_{B,M}A_{B,M}G_{B,M}$  white LEDs with wide-band red phosphors, as previously reported.<sup>15,17</sup>

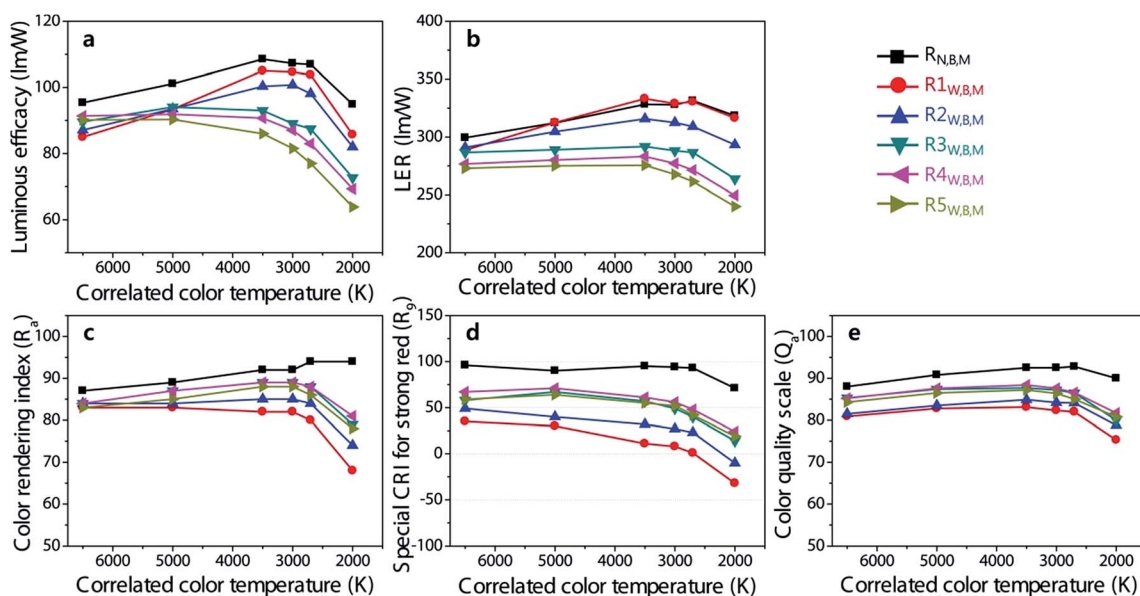


Fig. 6 The optical properties of the six combinations of four-package  $R_{B,M}A_{B,M}G_{B,M}$  white LEDs at different CCTs with the various red phosphors: (a) LE, (b) LER, (c) CRI, (d)  $R_g$ , and (e) CQS.

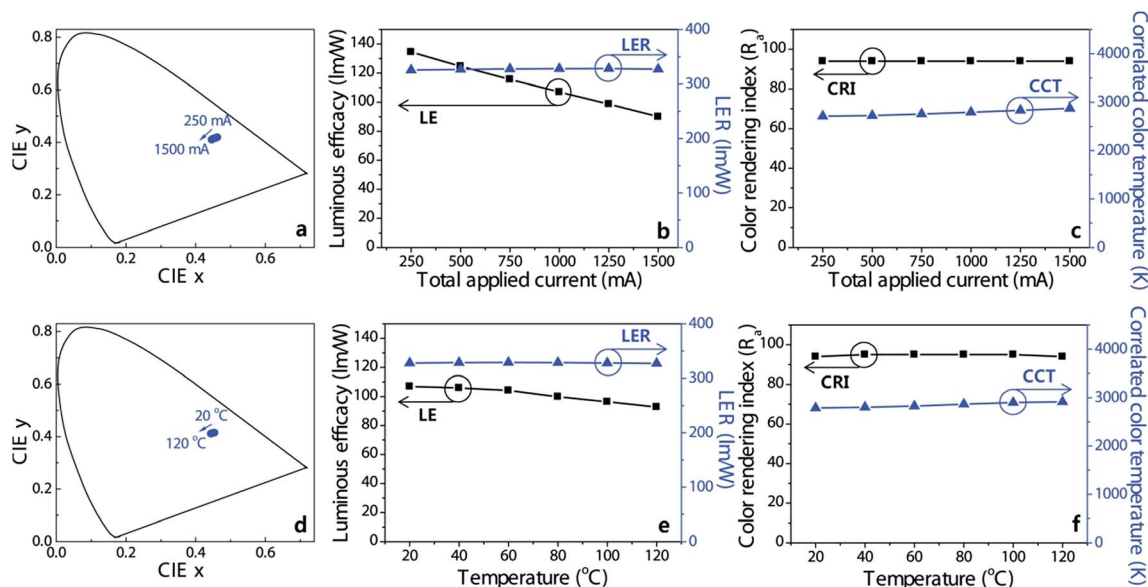


Fig. 7 Current dependence of the  $R_{N,B,M}A_{B,M}G_{B,M}B$  white LED at 2700 K at room temperature: (a) 1931 CIE color coordinates, (b) LE and LER, and (c) CRI and CCT. The temperature dependence of the  $R_{N,B,M}A_{B,M}G_{B,M}B$  white LED at 2700 K with a total applied current of 1000 mA: (d) 1931 CIE color coordinates, (e) LE and LER, and (f) CRI and CCT.

## 4. Conclusions

We synthesized a narrow-band red-emitting  $K_2SiF_6:Mn^{4+}$  phosphor using a facile etching method, and characterized the optical, crystal, morphological, and compositional properties of the  $K_2SiF_6:Mn^{4+}$  red phosphor using PLE/PL, XRD, and FE-SEM (EDS). As exhibited in the PL spectrum, the narrow-band red-emitting  $K_2SiF_6:Mn^{4+}$  phosphor emitted almost no photons above 700 nm wavelength, which does not influence the vision sensitivity and color discrimination of the human eye. Therefore, there are almost no wasted photons emitted from the narrow-band  $K_2SiF_6:Mn^{4+}$  phosphor for human vision and color perception. The simple combination of a narrow-band red-emitting  $K_2SiF_6:Mn^{4+}$  phosphor and a LPDF nano-multilayered film represents a simple method of realizing the most reddish monochromatic LED among all types of red LPDF-capped pc-LEDs in the CIE chromaticity diagram. The colors, performance levels, current stability, and temperature stability data of the narrow-band red-emitting pc-LEDs presented in this study confirm that the resultant red pc-LED can replace other red pc-LEDs that use the commercialized wide-band SCASIN red phosphor, although the relative QE of the prepared  $K_2SiF_6:Mn^{4+}$  phosphor is lower than those of the commercialized wide-band SCASIN phosphors. In order to compare the optical properties (LE, CRI,  $R_9$ , and CQS) of four-package white LEDs using a narrow-band  $K_2SiF_6:Mn^{4+}$  red pc-LED and five (Sr,Ca)AlSi<sub>3</sub>:Eu<sup>2+</sup> red pc-LEDs at the specified CCTs, we measured the four-package  $R_{B,M}A_{B,M}G_{B,M}B$  white LED by changing the red phosphor material type. When compared with the optical properties of the five  $R_{W,B,M}A_{B,M}G_{B,M}B$  white LEDs with wide-band red phosphors, the  $R_{N,B,M}A_{B,M}G_{B,M}B$  white LED including the narrow-band red phosphor exhibited high LE (107 lm W<sup>-1</sup>) and ultrahigh color qualities (CRI = 94,  $R_9$  = 93, and CQS = 93) at a

warm white CCT of 2700 K. Therefore, the  $K_2SiF_6:Mn^{4+}$  red phosphor is a good candidate for fabricating highly reddish monochromatic pc-LEDs and ultrahigh color quality warm white LED lighting. This approach, which develops a new type of narrow-band red-emitting  $K_2SiF_6:Mn^{4+}$  phosphor, deep red monochromatic pc-LED capped with LPDF, and a four-package white LED system with a blue semiconductor LED and R, G, A pc-LEDs, can lead to the development of ultrahigh color quality, tunable, smart lighting systems at warm white CCTs.

## Acknowledgements

This work was supported by the National Research Foundation of Korea (NRF) grant funded by the Korea government (MSIP) (no. 2011-0017449 and NRF-2012M1A2A2671718).

## References

- 1 E. F. Schubert and J. K. Kim, *Science*, 2005, **308**, 1274–1278.
- 2 M. H. Crawford, *IEEE J. Sel. Top. Quantum Electron.*, 2009, **15**(4), 1028–1040.
- 3 C.-C. Tu, J. H. Hoo, K. F. Böhringer, L. Y. Lin and C. Cao, *Opt. Express*, 2014, **22**(S2), A276–A281.
- 4 X. Li, J. D. Budai, F. Liu, J. Y. Howe, J. Zhang, X.-J. Wang, Z. Gu, C. Sun, R. S. Meltzer and Z. Pan, *Light: Sci. Appl.*, 2013, **2**, e50.
- 5 H. Wu, X. Zhang, C. Guo, J. Xu, M. Wu and Q. Su, *IEEE Photonics Technol. Lett.*, 2005, **17**(6), 1160–1162.
- 6 K. Sakuma, N. Hirosaki, N. Kimura, M. Ohashi, R.-J. Xie, Y. Yamamoto, T. Suehiro, K. Asano and D. Tanaka, *IEICE Trans. Electron.*, 2005, **E88-C**(11), 2057–2064.
- 7 C. Liao, R. Cao, Z. Ma, Y. Li, G. Dong, K. N. Sharafudeen and J. Qiu, *J. Am. Ceram. Soc.*, 2013, **96**(11), 3552–3556.

- 8 L. Lv, X. Jiang, S. Huang, X. Chen and Y. Pan, *J. Mater. Chem. C*, 2014, **2**, 3879–3884.
- 9 P. Pust, V. Weiler, C. Hecht, A. Tücks, A. S. Wochnik, A.-K. Henß, D. Wiechert, C. Scheu, P. J. Schmidt and W. Schinck, *Nat. Mater.*, 2014, **13**, 891–896.
- 10 A. A. Setlur, R. J. Lyons, J. E. Murphy, N. P. Kumar and M. S. Kishore, *ECS J. Solid State Sci. Technol.*, 2013, **2**(2), R3059–R3070.
- 11 W. Davis and Y. Ohno, *Opt. Eng.*, 2010, **49**, 216–225.
- 12 W. Davis and Y. Ohno, *Proc. SPIE*, 2005, **5941**, 59411G.
- 13 A. Žukauskas, R. Vaicekauskas, F. Ivanauskas, H. Vaitkevičius, P. Vitta and M. S. Shur, *IEEE J. Sel. Top. Quantum Electron.*, 2009, **15**(6), 1753–1762.
- 14 A. Žukauskas, R. Vaicekauskas and M. Shur, *Opt. Express*, 2010, **18**(3), 2287–2295.
- 15 J. H. Oh, S. J. Yang and Y. R. Do, *Light: Sci. Appl.*, 2014, **3**, e141.
- 16 P. F. Smet, A. B. Parmentier and D. Poelman, *J. Electrochem. Soc.*, 2011, **158**(6), R37–R54.
- 17 J. R. Oh, S.-H. Cho, J. H. Oh, Y.-K. Kin, Y.-H. Lee, W. Kim and Y. R. Do, *Opt. Express*, 2011, **19**(5), 4188–4198.
- 18 J. H. Oh, J. R. Oh, H. K. Park, Y.-G. Sung and Y. R. Do, *Opt. Express*, 2011, **19**(S3), A270–A279.
- 19 J. H. Oh, S. J. Yang, Y.-G. Sung and Y. R. Do, *Opt. Express*, 2012, **20**(18), 20276–20285.
- 20 T. Takahashi and S. Adachi, *J. Electrochem. Soc.*, 2008, **55**(12), E183–E188.
- 21 S. Adachi and T. Takahashi, *J. Electrochem. Soc.*, 2009, **12**(2), J20–J23.
- 22 R.-J. Xie, N. Hirotsaki, T. Takeda and T. Suehiro, *ECS J. Solid State Sci. Technol.*, 2013, **2**(2), R3031–R3040.